MRS Advances (2022) 7:410–414
https://doi.org/10.1557/s43580-021-00193-z

ORIGINAL PAPER

Magnetic nanoarrays on flexible substrates

Guinevere Strack[1] · Yassine AitElAoud[2] · Richard M. Osgood III[2] · Alkim Akyurtlu[1]

Received: 21 October 2021 / Accepted: 8 December 2021 / Published online: 23 January 2022

Abstract
In this work, we used nanosphere lithography to fabricate large area 2-D magnetic nanoparticle (MNP) arrays on a flexible polyimide substrate (Kapton). Samples were fabricated by assembling polystyrene (PS) spheres on thin films of Co capped with Au. Etched PS spheres were used to mask Co–Au particle arrays. The MNP arrays were subjected to superconducting quantum interference device measurements; flat samples (10 nm Co coated with 10 nm Au) exhibited an M_s of 117.3 emu g^{-1}, which was lower than the reported literature value for bulk Co (162.7 emu g^{-1}). When compared to the flat film, coercivity, H_c, increased in a linear fashion with respect to particle size. These preliminary results reveal that future investigations of the magnetic properties on flexible substrates should account for residual Co remaining in the polymeric material, the unique MNP shape, the effect of order (or lack or order) of the 2D array, and positioning with respect to the direction of the magnetic field.

Introduction

Magnetic nanoparticle (MNP) arrays have been shown to possess unique magneto-optical properties such as controlled magneto-optical resonance tuning [1]. Fabrication of MNP arrays of a few millimeters can be carried out using highly precise and costly techniques, such as e-beam lithography. In contrast, the high-throughput and low-cost technique of nanosphere lithography (NSL) can be used to fabricate large areas of ordered magnetic nanoparticle arrays on rigid or flexible substrates [2–12]. Flexible substrates are important in new application areas that require lightweight and conformal packaging for advanced electronics and electromagnetics functionalities. There are several variations to the NSL method, including masking and thermal approaches. Recently, our group has fabricated Au, Au–Co, and Co metallic nanoparticle arrays on Si wafer and flexible glass substrates. [2–4, 12, 13] In the thermal degradation approach, we applied heat or intense pulsed light (IPL) to degrade the polymer template, leaving behind an ordered nanoparticle array. [13] For the masking approach, closely packed polymeric spheres were assembled on top of the desired material/metal, the spheres were then reduced in size to produce isolated polymeric particles and then the metal layer was removed to reveal an ordered array. [2] Fabrication strategies for flexible arrays can be limited due to substrate properties such as temperature tolerance, chemical inertness, and outgassing under vacuum, therefore, we chose Kapton, which is a flexible substrate comprised of poly (4,4′-oxydiphenylene-pyromellitimide) that tolerates a wide temperature range and has a low outgassing rate under high vacuum.

Magneto-optical properties of nanostructures depend on the size, shape, composition, and spacing of the nanoparticles (NPs). [1] Magnetic properties such as saturation magnetization, M_s, and coercivity, H_c, are dependent on particle composition, size and shape. [7, 8, 11] The majority of the aforementioned publications focused on MNPs present fabrication strategies on ideal surfaces such as Si wafers. In our approach, we chose to apply the NSL process to a polyimide substrate, which, when compared to Si wafer, has the advantage of flexibility, and therefore extends the utility of the material to a wider range of applications. In this preliminary investigation, we measured the magnetic properties of Au-capped Co on Kapton, i.e., a non-ideal substrate.

✉ Guinevere Strack
Guinevere_Strack@uml.edu

✉ Alkim Akyurtlu
Alkim_Akyurtlu@uml.edu

[1] University of Massachusetts Lowell, Lowell, MA 01854, USA

[2] Optical and Electromagnetic Materials Team, US Army Combat Capabilities Development Command Soldier Center (DEVCOM Soldier Center), Natick, MA 01760, USA

Both flat Co films and MNP arrays were investigated using a superconducting quantum interference device (SQUID).

Experimental details

Sample fabrication

Fabrication of the flexible Au–Co arrays was carried out on Kapton (Dupont; ~ 1.5 inch squares). Initial cleaning was performed by rinsing the Kapton squares in isopropanol and DI water and then drying under N_2. Next, a 5 min oxygen plasma cleaning process was applied using the Oxford Dual Chamber Reactive Ion Etch Plasma Lab 80 Tool. Next, a layer of Co (10 nm) was deposited onto the clean Kapton using e-beam evaporation (CHA Industries). The Au layer (10 nm) was immediately deposited sequentially onto the Co without breaking vacuum. Then, polystyrene (PS) beads were assembled on top of the Co–Au via spin coating. A colloidal suspension of PS microspheres (10% solids; BangsLabs, USA) with an approximate diameter 200 or 500 nm was filtered through a syringe filter (cut-off = 1.5 µm) to remove large particles or 'supers' that could interfere with the assembly process. Next, the PS suspension was pipetted onto the Au and spun with a step-wise spin speed ramp [13]. These steps were 200 rpm for 5 s, 500 rpm 10 s, 1000 rpm for 20 s, 4000 rpm for 15 s, 6000 rpm for 10 s, 4000 rpm for 5 s, 1000 rpm for 5 s, 500 rpm for 5 s, and 200 rpm for 5 s. The PS bead-coated samples were placed in the Oxford RIE (50 W; 20 ccm) and etched for 0, or 60 s. The Au–Co layer was removed using an ICP Etch Tool (Oxford Plasmapro 380) in cryo cold mode (− 120 °C). Etching parameters were RF power of 100 W and an ICP power of 2000 W and an Ar flow rate of 20 ccm and an etch time of 90 s. Finally, the samples were subjected to high temperature (325 °C) for 3600 s under N_2 in a high-temperature oven (Blue M). Samples were stored in ambient conditions.

Please refer to the supplementary material section for sample characterization details (scanning electron microscopy (SEM) and superconducting quantum interference device (SQUID)).

Discussion

Sample fabrication

Flexible MNP arrays were fabricated on Kapton using the NSL process depicted in Fig. 1. First, clean Kapton was coated with a layer of Co and then a layer of Au was deposited using an e-beam evaporator without breaking vacuum. The Au layer was deposited to minimize oxidation of the Co layer and provide desired optical properties. Next, an assembled monolayer of filtered PS beads in aqueous suspension was applied on top of the Au surface via spin coating. Figure 2A depicts the hexagonal packing of the PS bead monolayer. After assembling the PS beads into a packed monolayer, the PS beads were etched to produce discrete islands blocking the metal layer. Partial removal of the PS bead mask during the oxygen plasma etch step reduces the size of the PS bead mask, as shown in Fig. 2B. The reduction in size of the polymer beads depends on the exposure time, i.e., long exposure times result in smaller bead masks. After the PS beads were reduced in size, the metal layer in areas not blocked by the PS bead mask was removed using ICP etching in cryo mode. The ICP etch tool was used in 'cryo mode' to minimize damage to the PS bead mask and to efficiently remove the Co–Au layer. The ICP etching process reduced

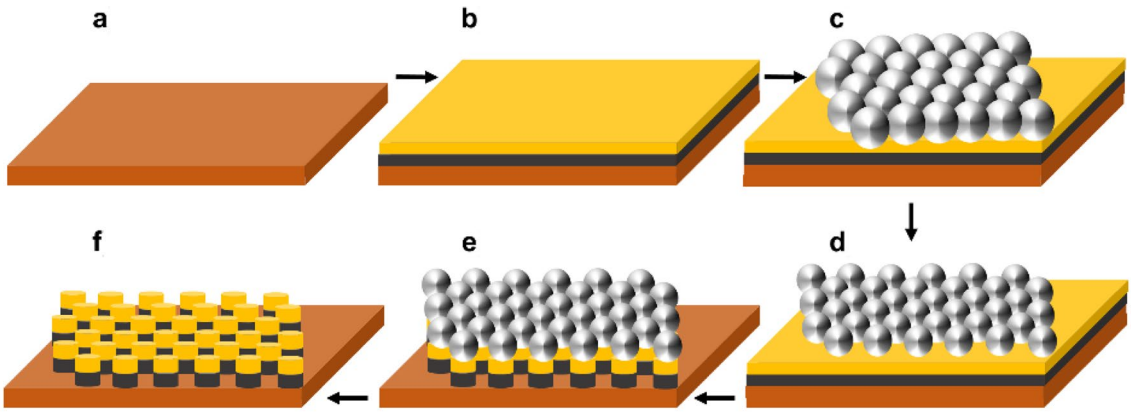

Fig. 1 Schematic depicting MNP fabrication processes based on NSL. The substrate is cleaned using IPA and O_2 plasma (**a**); 10 nm layers of Co and then Au are deposited onto the substrate via e-beam evaporation (**b**); the PS beads are assembled on the Co—Au layer via spin coating (**c**); the ordered PS beads are etched using O_2 plasma (**d**); the Co—Au layer is removed using ICP etching (**e**); and, finally, the PS beads are removed (**f**)

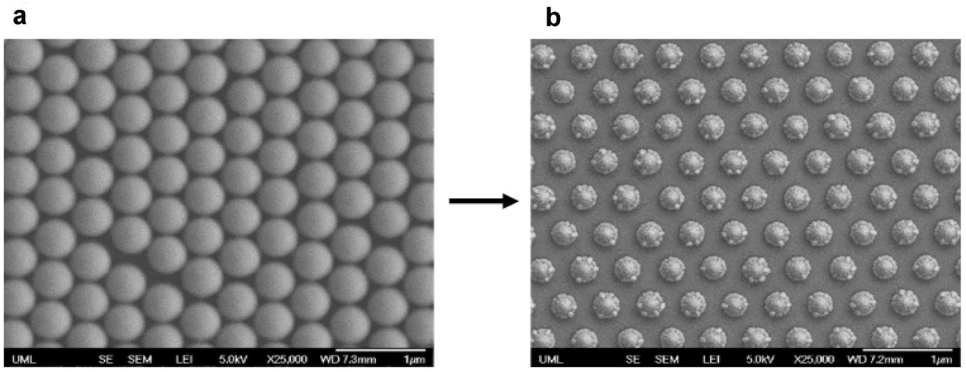

Fig. 2 SEM images of assembled PS beads before (**a**) and after (**b**) etching

the size of the PS beads without completely removing the bead mask. The remaining PS bead layer was removed to reveal a Co–Au particle array on flexible substrate, Fig. 3.

Sample characterization

SEM images of Co–Au particle arrays with average diameters of 115, 269, and 321 nm are displayed in Fig. 3, respectively. The particle arrays retained some of the original hexagonal ordering; however, the Kapton substrate is tentatively thought to distort the array due to inhomogeneity in the morphology and lack of stability during the fabrication process. Visual inspection confirmed that a metallic layer remained after the fabrication steps were performed, although the layer did not have a smooth reflective appearance associated with a continuous metallic film. The Samples without the PS bead mask were subjected to the fabrication process, and upon visual inspection, the metallic layer was not observable and the sample appeared to be a clean Kapton substrate.

SQUID measurements revealed that residual Co remained behind on the Kapton substrate that was subjected to the fabrication procedure without the PS bead mask. Figure 4A displays the hysteresis loops (H applied in the plane of the sample) for Co–Au-coated Kapton samples before and after the fabrication protocol. The hysteresis loop revealed that saturation magnetization, M_s, was 5–10% of the flat Co–Au film. Flat samples (10 nm Co coated with 10 nm Au) exhibited $M_s = 117.3$ emu g^{-1}, which was lower than the reported literature value (162.7 emu g^{-1}) by 27.9%. [14] It should be noted that the Co layer thickness (10 nm) is thin enough for properties to differ from bulk, and magnetic properties may be weaker very close to the interface. A reduction in magnetic saturation could be attributed to oxidized regions of Co, which could be a relatively large percentage for thin layers. M_s was obtained by estimating the mass of the Co in each sample. Given that there is residual Co remaining in the substrate, we expect that the mass has been underestimated, which can artificially inflate M_s. Magnetic hysteresis loops for Co–Au MNP arrays on Kapton were also obtained. When compared to the flat film, the coercivity, H_c, increased in a linear fashion with respect to particle diameter, Fig. 5. We considered the flat film as a particle array with $d = 0$. This linear increase occurred for the 2-D MNP arrays irrespective of the particle spacing or lack of ordering. This is tentatively associated with magnetic domains having roughly the same uniaxial in-plane anisotropy. [15]

Additional experiments were performed to understand if the hysteresis loops could be used for not only qualitative analysis, but to determine M_s. The saturation magnetization was obtained for 20 and 50 nm layers of Co and found to

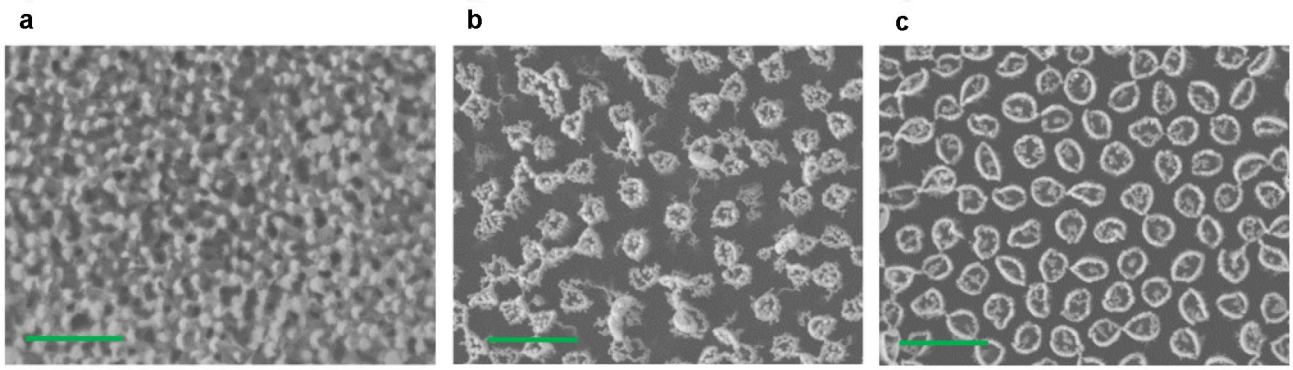

Fig. 3 SEM images of Co–Au MNP arrays on Kapton with average particle diameters of 155 (**a**), 269 (**b**), and 321 (**c**) nm. Scale bars = 1 μm

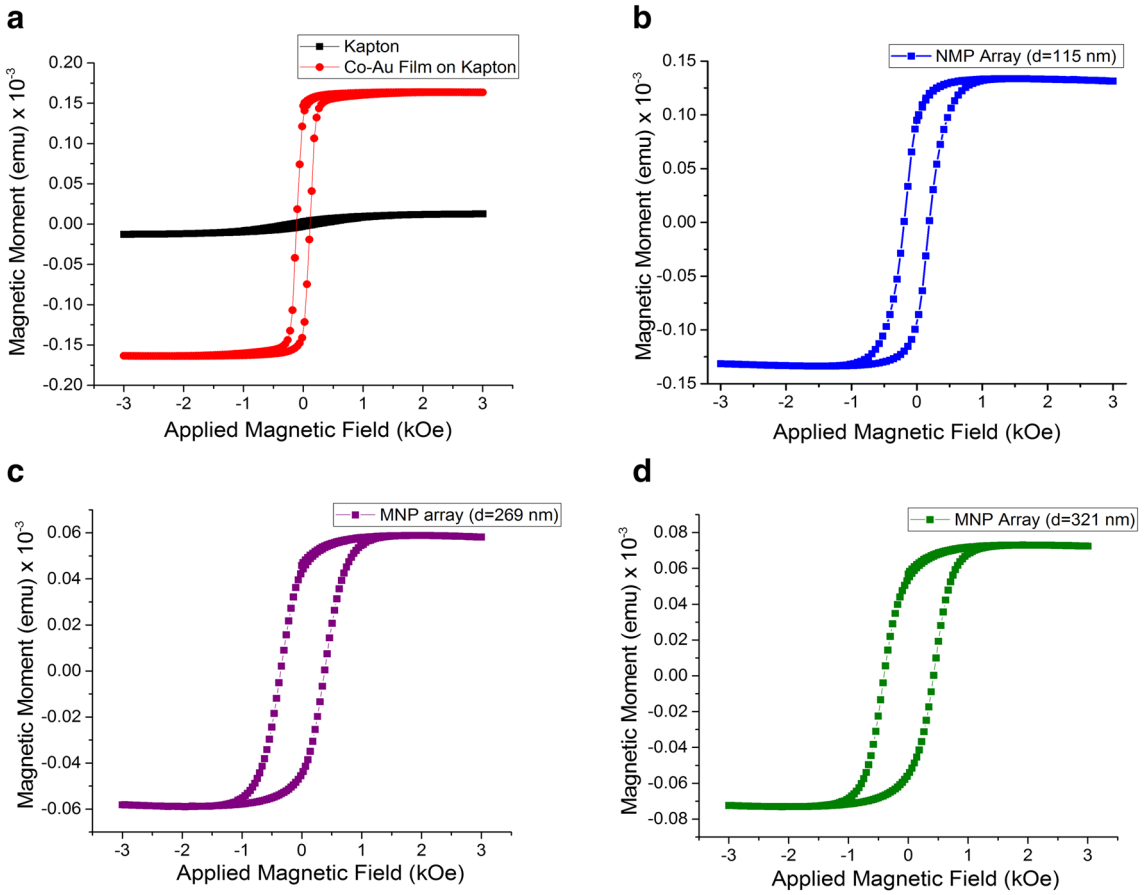

Fig. 4 Hysteresis loops (magnetic moment vs. applied magnetic field) of 4 × 4 mm samples of Kapton coated with a continuous layer of Co–Au (**a**) before (black) and after (red) Co–Au removal; NP arrays with particle diameters of 115 (**b**), 269 (**c**), and 321 (**d**) nm

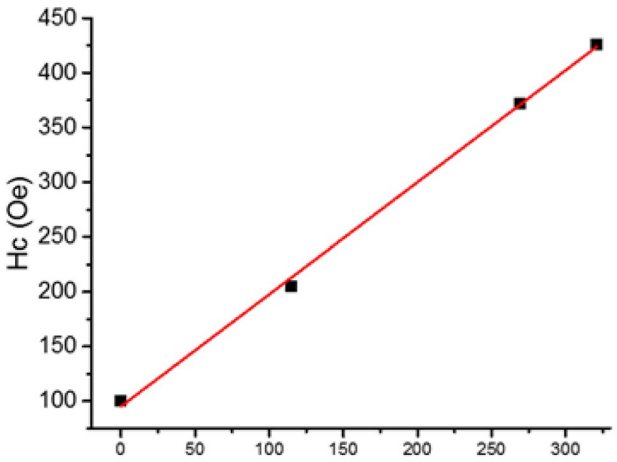

Fig. 5 Coercive field, H_c, with respect to particle diameter for Co films and MNP arrays on Kapton. Particle diameter of 0 is the flat film, which is comprised of 10 nm of Co coated with 10 nm of Au. MNP arrays were fabricated by using the flat film and removing a portion of the film to leave behind particle arrays

be 127.8 and 147.9 emu g^{-1}, 21.5% and 9.1% below the literature values, respectively. It should be noted that the 20 nm layer of Co was capped with Au, but the 50 nm layer was not capped. The saturation magnetization for the 50 nm layer of Co was obtained for the out-of-plane run and found to be140.5 emu g^{-1}. These results are much closer to the literature value for bulk Co. The experimentally obtained M_s values are listed in the table displayed in Figure SM1. M_s values for particle arrays were based on estimated residual Co mass, as depicted by SEM images. Given that residual Co remains behind on the bare Kapton sample, we have concluded that experimental methods that directly measure the remaining mass of Co should be employed in order to decouple the effects.

Conclusion

This preliminary investigation supports other published work demonstrating that magnetic properties (easy axis coercivity in this case) of particles with nanometric dimensions

are dependent on particle size. [7, 8, 11] Hysteresis loops obtained when the external magnetic field lay in the plane of the sample revealed that 2D MNPs exhibit increased H_c with respect to particle diameter. These preliminary results also revealed that future investigations of magnetic properties on flexible substrates should account for residual Co remaining in the polymeric material. The fabrication protocol, substrate material, and magnetic material will affect the properties and performance of the magnetic array. Moreover, the unique MNP shape, which is a flat disc, could have magnetic properties that deviate from spherical particles that are randomly distributed in a 3D space. Finally, the effect of order (or lack of order) in the 2D array should be taken into account along with bending, folding, and positioning with respect to the direction of the magnetic field.

Supplementary Information The online version contains supplementary material available at https://doi.org/10.1557/s43580-021-00193-z.

Acknowledgments We would like to thank Patrick Boisvert for assistance during the covid-19 shutdown with the SQUID magnetometer located at Massachusetts Institute of Technology Materials Research Laboratory.

Funding We are grateful for funding from the Assistant Secretary of the Army for Acquisition, Logistics and Technology (ASA(ALT)), and the DEVCOM Soldier Center Chief Scientist, whose programs funded this research through the DEVCOM Soldier Center–UML HEROES collaboration.

Data availability Data will be made available upon reasonable request.

Declarations

Conflict of interest On behalf of all authors, the corresponding author states that there is no conflict of interest.

References

1. M. Kataja, T.K. Hakala, A. Julku, M.J. Huttunen, S. van Dijken, P. Torma, Surface lattice resonances and magneto-optical response in magnetic nanoparticle arrays. Nat. Commun. **6**, 7072 (2015)
2. G. Strack, Y. AitElAoud, D. Slafer, R.M. Osgood III, A. Akyurtlu, Fabrication Strategies for Large-Area, Flexible Magnetic Nanoparticle Arrays. 2020 Virtual MRS Spring/Fall Meeting and Exhibit (Boston, MA, 2020)
3. G. Strack, Y. AitElAoud, R.M. Osgood III, A. Akyurtlu, Large-Area Active 2-D Metasurface Comprised of Magnetic Nanoparticles. 2019 MRS Fall Meeting and Exposition (Boston, MA, 2019).
4. G. Strack, Y. AitElAoud, R.M. Osgood III, A. Akyurtlu, Fabrication of Ordered Au–Co Nanoparticle Arrays. 2020 IEEE International Symposium on Antennas and Propagation and USNC-URSI Radio Science Meeting (Montreal, QB, 2020).
5. J.-R. Jeong, S. Kim, S.-H. Kim, J.A.C. Bland, S.-C. Shin, S.-M. Yang, Fabrication of hexagonal lattice Co/Pd multilayer nanodot arrays using colloidal lithography. Small **3**, 1529–1533 (2007)
6. S.M. Weekes, F.Y. Ogrin, W.A. Murray, Fabrication of large-area ferromagnetic arrays using etched nanosphere lithography. Langmuir **20**, 11208–11212 (2004)
7. F.Q. Zhu, Z. Shang, D. Monet, C.L. Chien, Large enhancement of coercivity of magnetic Co/Pt nanodots with perpendicular anisotropy. J. Appl. Phys. **101**, 09J101 (2007)
8. P. Tiberto, F. Celegato, G. Barrera, M. Coisson, F. Vinai, P. Rizzi, Magnetization reversal and microstructure in polycrystalline Fe50Pd50 dot arrays by self-assembling of polystyrene nanospheres. Sci. Technol. Adv. Mater. **17**, 462–472 (2016)
9. D.-G. Choi, S. Kim, S.-G. Jang, S.-M. Yang, J.-R. Jeong, S.-C. Shin, Nanopatterned magnetic metal via colloidal lithography with reactive ion etching. Chem. Mater. **16**, 4208–4211 (2004)
10. W.G. Wang, A. Pearse, M. Li, S. Hageman, A.X. Chen, F.Q. Zhu et al., Parallel fabrication of magnetic tunnel junction nanopillars by nanosphere lithography. Sci. Rep. **3**, 1948 (2013)
11. X. Li, Z.R. Tadisina, S. Gupta, G. Ju, Preparation and properties of perpendicular CoPt magnetic nanodot arrays patterned by nanosphere lithography. J. Vac. Sci. Technol., A **27**, 1062–1066 (2009)
12. G. Strack, A. Akyurtlu, Fabrication of Ordered Au–Co Nanoparticle Arrays. 2020 IEEE International Symposium on Antennas and Propagation and USNC-URSI Radio Science Meeting (Montreal, QB, 2020).
13. G. Strack, Y. AitElAoud, R.M. Osgood III, A. Akyurtlu, Large area nanoparticle arrays and method of making thereof (2020).
14. J.I. Schwerdt, G.F. Goya, M.P. Calatayud, C.M. Fau, C.B. Hereñú, H.C. Fau, P.C. Reggiani, R.P. Fau, R.G. Goya, R.G. Goya, Magnetic field-assisted gene delivery: achievements and therapeutic potential **12**(2), 116–126 (2012).
15. B.D. Cullity, C.D. Graham, *Introduction to Magnetic Materials*, 2nd edn. (IEEE Press, Hoboken, 2009)